

Automatic Detection of Focal Arteriolar Narrowing from Color Retinal Image

Pallab Kanti Roy, Alauddin Bhuiyan, Kotagiri Ramamohanarao

Abstract—In this paper an automated method is presented for the detection of Focal Arteriolar Narrowing (FAN), a precursor for hypertension, stroke and other cardiovascular diseases. Our contribution in this paper is that, we have proposed a novel retinal blood vessel tracing and vessel width measurement algorithm, which is fully automated. We developed a novel method to detect FAN affected vessel segments by analysing their width distribution pattern. For initial results and quantitative evaluation of the proposed method, we evaluate our method on 30 color retinal images which are randomly selected by an experienced grader from SiMES dataset. We achieved the sensitivity of 75% and specificity of 98% in detecting FAN affected vessel segments and sensitivity of 80% and specificity of 86% in identifying healthy and FAN affected images. The acquired result shows the potential suitability of the proposed method for assisting the ophthalmologist to detect the FAN in clinical practice.

I. INTRODUCTION

The number of patients suffering from cardiac and cerebrovascular disease is increasing day by day. Recent research suggests that retinal Focal Arteriolar Narrowing (FAN) has a significant association with cardiac and cerebrovascular diseases like hypertension, diabetes, coronary heart disease and stroke [1]. These are the leading causes of death in developed and developing countries, and imposes an enormous socio-economic burden on the community [2]. This figure is expected to increase due to the ageing population and cardiovascular risk factors such as diabetes and obesity. Identification of high-risk but asymptomatic people at an early stage holds the key to allow timely implementation of preventative strategies (e.g., diet, physical exercise) and medical interventions (e.g., cholesterol lowering drugs) to prevent these diseases effectively.

Focal arteriolar narrowing (FAN) is the sudden narrowing of arteriolar width in the retina (see Fig. 1). In recent years, a number of researches [3] have been published which shows significant correlation between FAN, hypertension and cardiovascular diseases (CVDs). However, these studies assess FAN qualitatively which rely on grader's subjective assessment. This qualitative assessment, however, is a subjective process as it depends on the grader's expertise and thus, it has many limitations, such as accuracy and reproducibility. Moreover, it is a tedious and time-consuming process, which

hinders the assessment to be done on large-scale screening for FAN detection. Therefore, an automated system is a necessity for accurate detection and quantification of FAN. In this paper, we aim to address this automatic detection of FAN in the color retinal images.

L.Pedersen et al. [4] has presented a semi-automated method for the detection of FAN. Based on the user given vessel profile starting and ending point they use Dijkstra's shortest path algorithm to find a trace inside the vessel and its direction. The vessel diameter is estimated as the width of the intensity profile and they analyse the pattern of the vessel width increase and decrease to detect FAN. Another method on FAN detection is proposed by Yuji Hatanaka et al. [5]. In their method they divided the blood vessels based on the position of the branch and crossover points. Then they measure the diameter of the detected blood vessels. They detected a vessel as abnormal if its diameter in any section is narrower than two third of the average diameter.

Very little work has been done on the automatic detection of FAN. Therefore, huge improvement is necessary for automated screening of FAN in the retinal image with automated vessel segmentation, vessel fragmentation based on the landmark points and measurement of vessel fragment's width to identify and quantify FAN. In this paper, we address these issues.

The rest of the paper is organized as follows. Section II details the FAN detection technique. The experimental results are presented in section III. Discussions and conclusions are presented in Section IV.

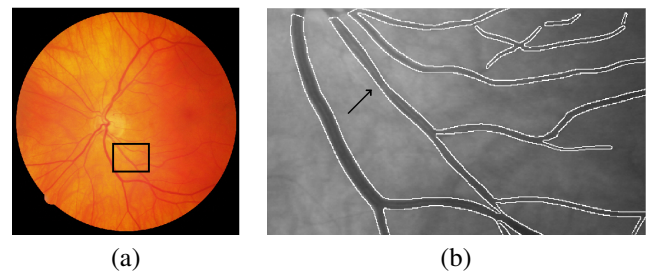


Fig. 1. From left to right: (a) Color Retinal Image with Focal Arteriolar Narrowing (FAN) (b) Cropped region of FAN

II. METHODOLOGY

Our proposed method (Fig. 2) has 6 steps : (1) image preprocessing for noise reduction and image enhancement; (2) vessel segmentation, vessel centerline computation and optic disc detection from preprocessed and normalized retinal

Pallab Kanti Roy is with the Department of Computing and Information Systems, The University of Melbourne, VIC 3010, Australia, e-mail: roypp@student.unimelb.edu.au.

Alauddin Bhuiyan is with the ICT Centre, Commonwealth Scientific and Industrial Research Organization (CSIRO), Australia.

Kotagiri Ramamohanarao is with the Department of Computing and Information Systems, the University of Melbourne, Australia.

image; (3) bifurcation/branch and crossover point detection from vessel centerline image; (4) vessel fragmentation based on the position of branch and crossover points; (5) vessel fragment's width measurement; (6) focal arteriolar narrowing detection from the width pattern of the vessel fragment. At first, Gabor filter is applied to analyse the texture and obtain features for vessel segmentation. Then unsupervised clustering algorithm i.e., Otsu's method is applied to segment the blood vessels. Following this, morphological skeletonization operation is applied to obtain the vessel centerline. We use the position of the branch and crossover points to fragment vessel centerline image. We use optic disk center and move around it in a circular path to map the fragmented vessel segments. Vessel width is computed from fragmented vessel centerline image and binary vessel segmented image. Once we compute the width vector for each vessel fragment. We calculate mean, standard deviation of the width of each vessel fragment. Then we apply a threshold on the mean and standard deviation of the the width to identify the potential FAN affected vessel fragments. After selecting potential FAN vessel fragments we calculate FAN weight for each of them. Finally we apply a threshold on this FAN weight to detect FAN affected vessel fragment.

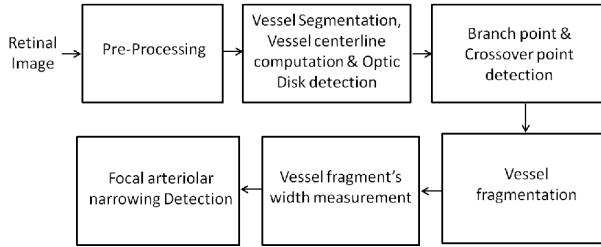


Fig. 2. Block diagram of the proposed method .

A. Preprocessing and Image Normalization

The green channel of the image is filtered using a 3x3 median filter to remove occasional salt-and-pepper noise. Further noise removal is performed by convolving the image with gaussian filter. Region growing and feature calculation is made more reliable by this step. The background intensity, denoted as B , is estimated by applying a 11x11 median filter. Here I represents the original green channel image. A shade corrected image is generated with $S' = I/B - 1$ and is normalized for global image contrast by dividing its standard deviation, $S = S'/std(S')$.

B. Vessel Segmentation and Optic Disk detection

As vessel have a special texture pattern which is different from the background, we apply texture analysis based vessel segmentation. A Gabor filter has weak responses along all orientations on the smooth (background) surface. On the other hand, when it is positioned on a linear pattern object (like a vessel) the Gabor filter produces relatively large differences in its responses when the orientation parameter changes [6]. A set of textures was obtained based on the use of Gabor filters according to a multichannel filtering

scheme. For this purpose, each image was filtered with a set of Gabor filters with different preferred orientation, spatial frequencies and phases. The filter results of the phase pairs were combined, yielding the Gabor energy quantity [7]:

$$E_{\xi,\eta,\Theta,\lambda} = \sqrt{r_{\xi,\eta,\Theta,\lambda,0}^2 + r_{\xi,\eta,\Theta,\lambda,\pi/2}^2}$$

where $r_{\xi,\eta,\Theta,\lambda,0}^2$ and $r_{\xi,\eta,\Theta,\lambda,\pi/2}^2$ are the outputs of the symmetric and antisymmetric filters. We used Gabor energy filters with twenty-four equidistant preferred orientations ($\Theta = 0, 15, 30, \dots, 345$) and three preferred spatial frequencies ($\lambda = 6, 7, 8$). In this way an appropriate coverage was performed of the spatial frequency domain. We considered the maximum response value per pixel on each color channel to reduce the feature vector length and complexity of training on data for the classifier. We applied thresholding based pixel clustering method which is based on the well-known Otsu's thresholding method [8]. After creating the binary segmentation of retinal blood vessels we apply the morphological skeletonisation operation on the binary vessel segmented image to extract the vessel centerlines. We use [9] for optic disk detection and its center computation. In this method optic disk is detected based on its geometrical features and intensity information.

C. Bifurcation and Crossover Point Detection

We apply a method proposed in [10] on the vessel centreline image to detect the potential bifurcation and crossover points. The geometrical and topological properties of the blood vessels passing through these points are utilized to identify these points as the vessel bifurcations and crossovers.

D. Vessel fragmentation

Based on the position of the branch and crossover points we first divide the blood vessels into fragments. Then we remove vessels in the optic disk region from fragmented vessel centerline image. This is because we can not measure width of this regions. To map the connected vessel fragments outside of the optic disk region we move around the center of the optic disk in a circular path. We initially set the optic disk's diameter as the radius of the circle to traverse. Whenever we find a centerline pixel we set this as the start point of the region growing technique [11] to traverse the centerline pixels until map the end point. After mapping a connected centerline vessel fragment we store its centerline points and flag them to avoid considering them again. We increase the radius of the circle by 5 and continue this process until we reach the boundary of the retinal image. After completing this vessel fragment searching we have a database of connected vessel fragment's centerlines. We consider those vessel fragments which have a length ≥ 30 pixels. Then we measure the width of those vessel fragments to compute potential FAN vessels as shown in Fig .3.

E. Measurement of vessel width

In theory, vessel calibre or width is the shortest linear distance which passes through the vessel center. For this,

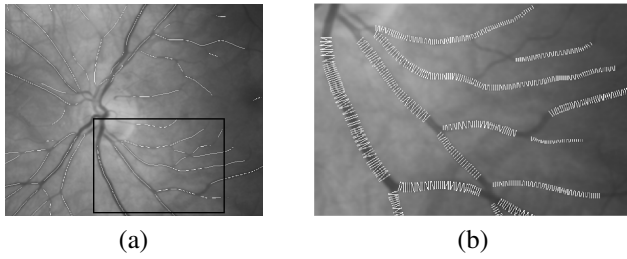


Fig. 3. Automatic vessel fragmentation and width measurement (from Left to Right): (a) Automatic vessel fragmented Image,(b) Automatic width measurement of vessel fragments.

each of the centerline pixel's of potential vessel fragment is considered to obtain pixel location on the left and the right side of the centerline which are at a certain normal distance from the centerline pixel positioned in vessel edge and represent the width (Fig. 4). Each centerline pixel and another short distance pixel in the centerline are considered as the line end-points. The slope and actual direction of the line are computed to find the perpendicular points on both sides of the current centerline pixel. The method is as follows: Let, (X_1, Y_1) and (X_2, Y_2) be two points in the centerline which are considered as the line end-points. The left side point (L_x, L_y) and right side point (R_x, R_y) for (X_2, Y_2) are computed as follows:

$$\begin{aligned} L_x &= X_2 - r * \sin(\theta + \frac{\pi}{2}) \\ L_y &= X_2 + r * \cos(\theta + \frac{\pi}{2}) \\ R_x &= X_2 - r * \sin(\theta + 3 * \frac{\pi}{2}) \\ R_y &= X_2 + r * \cos(\theta + 3 * \frac{\pi}{2}) \end{aligned}$$

Here r is the normal distance from the point (X_2, Y_2) and θ is the actual angle in the image which is computed from the slope and direction of the line considering two points (X_1, Y_1) and (X_2, Y_2) . Initially we set the value of r as 1. Then we check the vessel segmented image for white pixel in these positions. We increase the normal distance r and check for white pixel until we reach in the black pixels or background. We note that we consider the final white pixel position as the width point. After finding the boundary vessel pixels on both side of a centerline point we calculate euclidean distance between them and use this distance as width of the vessel fragment with respect to this centerline point. When we find the vessel width for a centerline point, we move to next centerline point. We continue this process until we reach the end point of a vessel fragment.

F. Detection of focal arteriolar narrowing

For each vessel fragment we have a number of widths, we calculate mean, standard deviation and FAN weight from these widths of each vessel fragment. Then we filter the vessel fragments in two steps to detect FAN as follows. In step one, we select those vessel fragments for which $3mm \leq$

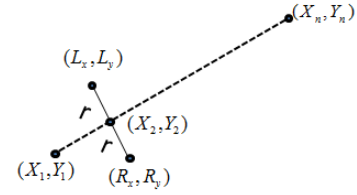


Fig. 4. Mapping the points on left side (L_x, L_y) and right side (R_x, R_y) of a centerline pixel.

$Mean\ Width \leq 7mm$ and $Standard\ Devtion\ of\ Width \geq 1.5$. We empirically select the threshold value for the mean and standard deviation of the width to select the potential arteries. Applying this threshold we first identify the vessel fragments that have abnormal narrowing or widening. In step two, we detect FAN affected vessel based on their width pattern. FAN affected vessel fragment have a special width pattern as shown in Fig. 5 & 6.

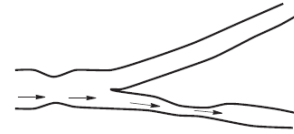


Fig. 5. Example of a vessel with Focal Arteriolar Narrowing (FAN).

In a FAN affected (Fig. 5) vessel fragment, width distribution follows a special pattern where normal width distribution is followed by a decrease in the width and then again it becomes normal width. To detect this pattern we first divide the vessel fragment into some non-overlapping windows of length five (Fig. 6). We calculate the mean width for each window. Then we find a window that has the minimum width and comparing with atleast two windows before and after it. Let assume, $W3$ is the selected window which has minimum mean width. $W1$ and $W2$ are two consecutive windows before it and $W4$ and $W5$ are two consecutive windows after it. We calculate the FAN weight for this vessel fragment from the mean width of these windows as follows:

$$\begin{aligned} g1 &= |w3 - w1| + |w3 - w2| \\ g2 &= |w3 - w4| + |w3 - w5| \end{aligned}$$

$$W = \alpha * g1 + \beta * g2 + \gamma * \exp -(|g1 - g2|)$$

From the experimental observation of our dataset we select $\alpha = 0.25$, $\beta = 0.25$ and $\gamma = 0.50$.

Finally we select those vessels as FAN affected vessel which have FAN weight $W \geq 5$. Fig. 7 shows a FAN affected vessel fragment and it's automatic detection.

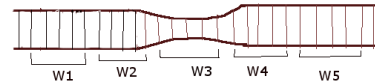


Fig. 6. Dividing vessel fragment into non-overlapping window of length 5.

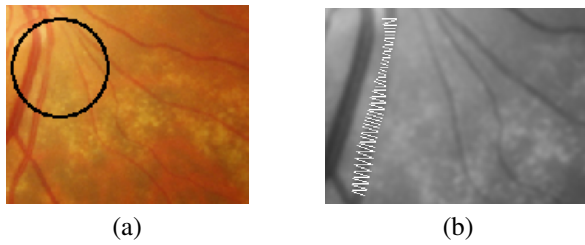


Fig. 7. Automatic Detection of Focal Arteriolar Narrowing (from left to right): (a) Cropped portion of a FAN affected vessel (b) Automatic Detection of FAN from the width of vessel fragments.

III. RESULTS

Thirty color retinal images randomly obtained from a population based study, the Singapore Malay Eye Study (SiMES) [3], are tested by the proposed method. These color retinal images were captured with the Canon D-60 digital fundus camera. Each image resolution was 3072x2048 pixels with one pixel stands for 5.11 microns in magnification. The images are selected by an experienced grader at the Australian E-Health Research Centre, Commonwealth Scientific and Industrial Research Organization, Perth, Australia. For evaluation we test the accuracy of the method on vessel level and image level. In these images we analyse all 1530 vessel fragments. Among them 12 vessel fragments are identified as FAN affected by our expert grader. Our proposed method detected 37 vessel fragments out of 1530 as FAN affected. Among them 9 vessel fragments were originally found to be FAN affected. Our method detected 1493 vessel fragments as normal among them FAN was found in 3 vessel fragments. We used sensitivity and specificity to measure the accuracy of our method. FAN vessel-fragment is considered as positive; if correctly detected true positive (TP) and if not false positive (FP). Similarly normal vessel-fragment is considered as Negative; if correctly detected true negative (TN) and if not false negative (FN). We used the following formula and computed the sensitivity and specificity:

$$Sensitivity = \frac{TP}{(TP + FN)}$$

$$Specificity = \frac{TN}{(TN + FP)}$$

Our proposed method achieved 75% sensitivity and 98% specificity in detecting FAN affected vessel fragments.

In image level, our method detected FAN in 11 images, among them 8 images were identified as FAN affected by the grader. In the remaining 19 images which were identified as normal by our proposed method, 17 images were detected as normal by the grader. Our proposed method achieved 80% sensitivity and 86% specificity in identifying healthy and FAN affected images.

IV. DISCUSSIONS AND CONCLUSIONS

We have presented a novel algorithm to detect focal arteriolar narrowing (FAN). In this paper our contributions

are : (a) development of a novel retinal vessel tracing and fragmentation algorithm which is fully automatic; (b) development of a technique for retinal vessel width measurement; and (c) development of a new method to detect the pattern of the width distribution of FAN affected vessel fragment. The results obtained from the preliminary work performed on 30 images shows good sensitivity and specificity as mentioned in the result section. However, we face some challenges in the course of testing the scheme. Some vessel segment seems broken after the binary vessel segmentation because of their lower contrast. A robust vessel contrast enhancement technique is required to overcome this problem. At present, we are working on improving the scheme to quantify the severity of FAN. In future, we will include more clinical cases in our method to analyse the properties of FAN more elaborately. The technique proposed in this paper will help to improve the detection accuracy and it will reduce the workload of ophthalmologist in the future.

REFERENCES

- [1] T.Y. Wong, R. Klein, A.R. Sharrett, D.J Couper, J.M. Tielsch, B.E.K Klein and L.D Hubbard, Retinal arteriolar narrowing and risk of coronary heart disease in men and women, JAMA: the journal of the American Medical Association, vol. 287, no. 9, pp. 1153-1159, 2002.
- [2] Global atlas on cardiovascular disease prevention and control, http://www.who.int/cardiovascular_diseases/en/, [Online; accessed 01-02-2013].
- [3] T.Y. Wong, R. Klein, A.R. Sharrett, B.B. Duncan, D.J. Couper, BE Klein, L.D. Hubbard, F.J. Nieto, et al., Retinal arteriolar diameter and risk for hypertension, Annals of internal medicine, vol. 140, no. 4, pp. 248, 2004.
- [4] L. Pedersen, M. Grunkin, B. Ersboll, K. Madsen, M. Larsen, N. Christoffersen and U. Skands, Quantitative measurement of changes in retinal vessel diameter in ocular fundus images, Pattern Recognition Letters, vol. 21, no. 13, pp. 1215-1223, 2000.
- [5] Y. Hatakana, T. Nakagawa, Y. Hayashi, A. Aoyama, X. Xhou, T. Hara, H. Fujita, Y. Mizukusa, A. Fujita, and M. Kakogawa, Automated detection algorithm for arteriolar narrowing on fundus image, In 27th annual conference on Engineering in Medicine and Biology Society, IEEE-EMBS, pp. 286-289, 2005.
- [6] D. Wu, M. Zhang, J.C. Liu and W. Bauman, On the adaptive detection of blood vessels in retinal images, IEEE Transactions on Biomedical Engineering, vol. 53, no. 2, pp. 341-343, 2006.
- [7] P. Kruijzinga, N. Petkov and SE Grigorescu, Comparison of texture features based on Gabor filters, In International conference on Image analysis and processing, IEEE, pp. 142-147, 1999.
- [8] N. Otsu, A threshold selection method from gray level histogram, IEEE Trans Syst Man Cybern, vol. 9, pp. 62-66, 1992.
- [9] A. Bhuiyan, R. Kawasaki, T.W. Wong and R. Kotagiri, A New and Efficient Method for Automatic Optic Disc Detection Using Geometrical Features, In World Congress on Medical Physics and Biomedical Engineering, Munich, Germany, pp. 1131-1134, 2010.
- [10] A. Bhuiyan, B. Nath, J. Chua and K. Ramamohanarao, Automatic detection of vascular bifurcations and crossovers from color retinal fundus images, In 2007 3rd International conference on Signal-Image Technologies and Internet-Based System (SITIS), IEEE, pp. 711-718.
- [11] R C Gonzalez and R E Woods, Digital Image Processing, 3rd Edition, Pearson Prentice Hall, 2008.